Journal of Photochemistry & Photobiology, B: Biology 168 (2017) 98–106

Contents lists available at ScienceDirect

Journal of Photochemistry & Photobiology, B: Biology

journal homepage: www.elsevier.com/locate/jphotobiol

Spontaneous ultra-weak photon emission in correlation to inflammatory metabolism and oxidative stress in a mouse model of collagen-induced arthritis

Min He [a,b], Eduard van Wijk [a,b,e,f,*], Herman van Wietmarschen [a,b,d], Mei Wang [a,b,c,f], Mengmeng Sun [a,b,f], Slavik Koval [a], Roeland van Wijk [b,e], Thomas Hankemeier [a,b], Jan van der Greef [a,b,d]

[a] Analytical BioSciences, LACDR, Leiden University, P.O. Box 9502, 2300 RA Leiden, The Netherlands
[b] Sino-Dutch Center for Preventive and Personalized Medicine, Leiden University, P.O. Box 9502, 2300 RA Leiden, The Netherlands
[c] SU Biomedicine, Utrechtseweg 48, 3700 AJ Zeist, The Netherlands
[d] TNO, P.O. Box 360, 3700 AJ Zeist, The Netherlands
[e] Meluna Research, Geldermalsen, The Netherlands
[f] Changchun University of Chinese Medicine, No. 1035, Boshuo Rd, Jingyue Economic Development District, Changchun 130117, China

ARTICLE INFO

Article history:
Received 2 September 2016
Received in revised form 22 December 2016
Accepted 23 December 2016
Available online 3 February 2017

Keywords:
Collagen-induced arthritis
Correlation networks
Systems biology
Metabolomics
Ultra-weak photon emission

ABSTRACT

The increasing prevalence of rheumatoid arthritis has driven the development of new approaches and technologies for investigating the pathophysiology of this devastating, chronic disease. From the perspective of systems biology, combining comprehensive personal data such as metabolomics profiling with ultra-weak photon emission (UPE) data may provide key information regarding the complex pathophysiology underlying rheumatoid arthritis. In this article, we integrated UPE with metabolomics-based technologies in order to investigate collagen-induced arthritis, a mouse model of rheumatoid arthritis, at the systems level, and we investigated the biological underpinnings of the complex dataset. Using correlation networks, we found that elevated inflammatory and ROS-mediated plasma metabolites are strongly correlated with a systematic reduction in amine metabolites, which is linked to muscle wasting in rheumatoid arthritis. We also found that increased UPE intensity is strongly linked to metabolic processes (with correlation co-efficiency $|r|$ value >0.7), which may be associated with lipid oxidation that related to inflammatory and/or ROS-mediated processes. Together, these results indicate that UPE is correlated with metabolomics and may serve as a valuable tool for diagnosing chronic disease by integrating inflammatory signals at the systems level. Our correlation network analysis provides important and valuable information regarding the disease process from a system-wide perspective.

1. Introduction

Rheumatoid arthritis (RA) is one of the most prevalent chronic autoimmune diseases, occurring in about approximately 1% of the population in Western countries [1,2]. RA manifests as a complex inflammatory syndrome that typically includes joint swelling, pain, and hyperthermia, as well as synovial hyperplasia and destruction of cartilage and bones in the joints. RA is considered a systemic disease that is caused by a variety of pathophysiological processes [3]. These processes are accompanied by increased levels of cytokines such as tumor necrosis factor α (TNF-α) and interleukins (IL-1β and IL-6) in the blood and interstitial fluids, activation of NF-κB pathways (to inhibit apoptosis in various immune cells), and systemic disruptions in inflammatory metabolite synthesis [4–6].

Experimental studies of RA—particularly the pathophysiological mechanisms of therapeutic interventions—are often conducted using animal models. The most commonly used model for RA is the collagen-induced arthritis (CIA) mouse model, which has pathophysiological processes and features similar to patients with RA [7–11]. In addition, advances in metabolomics technology, which now enable researchers to measure extremely low concentrations of metabolites in several pathways simultaneously [12], has facilitated the study of RA in considerably more detail, thereby increasing our understanding of the pathological mechanisms that underlie the disease [13]. We previously studied the differences in molecular profiles between CIA mice and control mice by examining differences with respect to inflammation and reactive oxygen species (ROS), analyzed using univariate and multivariate metrics [14]. In addition to the well-characterized inflammatory phenomenon, issues related to muscle wasting and energy expenditure

* Corresponding author at: Analytical BioSciences, LACDR, Leiden University, P.O. Box 9502, 2300 RA Leiden, The Netherlands.
E-mail address: eduard.vanwijk@sinodutchcentre.nl (E. van Wijk).

http://dx.doi.org/10.1016/j.jphotobiol.2016.12.036
1011-1344/

are also present in RA [15–18], and this is reflected by the presence of amine metabolites in the plasma of CIA mice [19].

Differences between CIA mice and control mice were also observed with respect to the intensity of ultra-weak photon emission (UPE), which reflects differences in the organization of the system at a biophysical level [20]. UPE is a process that occurs in all living organisms and is the spontaneous emission of light with extremely weak intensity (10^1–10^3 photons/s/cm^2) in the UV, visible, and near-IR spectra [21]. Many studies have focused on the relationship between UPE and ROS production during metabolic processes [22–26]. Considering that ROS production is closely associated with inflammatory diseases and impaired metabolic processes, it is reasonable to expect that UPE is also associated with inflammatory disease and/or metabolic processes. UPE might therefore be used to help diagnose inflammation and inflammation-related diseases. UPE has been proposed for monitoring lipid peroxidation in cell membranes [27], and applications using UPE in human studies—and their potential relationship with ROS—were summarized by van Wijk [23]. Moreover, the putative relationship between UPE, physiological state, and metabolic processes has been proposed by several research groups [28–31]. Here, we performed an integrated analysis of the biochemical and biophysical differences between CIA mice and control mice, based on the hypothesis that a combined analysis would reveal unique insight into the biochemical and biophysical changes that occur during RA.

Network biology is an emerging field in biomedical research, and network biology tools are increasingly used to identify clusters of correlated parameters, to visualize or explore high-dimensional data, and to understand or interpret interactions that reflect part of a complex biological system [32,33]. Correlation networks have been used in "omics" studies to combine complex data sets, for example combinations of metabolomics, genomics, and/or proteomics data sets. Correlation networks are also used to support the biological interpretation of large data profiles and to differentiate disease phenotypes [34–37]. Here, we expanded the systems-based approach of correlation-based analyses in order to examine the relationship between metabolomics profiling and UPE data. Using this correlation network analysis, we visualized systematic perturbations in bio-photons, inflammatory processes, and ROS-related mediators. This approach may be used to facilitate the diagnosis of disease and/or to discriminate between disease syndromes, particularly with respect to complex chronic diseases such as RA and type 2 diabetes mellitus.

2. Materials and Methods

2.1. Animal Study Samples, Modelling, and Ethics Statement

CIA was induced by the intraperitoneal injection of type II collagen and lipopolysaccharide in adult (6–7 weeks of age) DBA/1 J male mice as described previously [38]; the CIA and control (Ctrl) groups contained 10 mice each. The injections were performed on days 0, 14, 28, 42, and 56; UPE intensity was then measured in each paw (day 70th), and blood was collected into pre-cooled EDTA tubes (BD Vacutainer, Plymouth, UK) immediately after UPE measurements. The blood samples were centrifuged at 3000 × *g* for 10 min, and then stored at −80 °C until metabolic measurements were performed [14]. All animal experiments were performed in compliance with the Guide for the Care and Use of Laboratory Animals (National Institutes of Health, Bethesda, MD). All animal care and experiments were approved by the Tohoku Institute of Technology Research Ethics Committee, Sendai, Japan.

2.2. Instruments and Data Acquisition

2.2.1. UPE Instruments and Settings

UPE was measured using a 600 series CCD camera system (Spectral Instruments, Inc., Tucson, AZ) equipped with a closed-cycle mechanical cryogenic unit (held at −120 °C) as the cooling system. Prior to the UPE measurement, mice were maintained in controlled dark conditions. The detailed settings of the CCD system including figures about the measured location on mice is described in Van Wijk et al. [20]. In brief, the CCD camera with 2048 × 2048 pixel resolution and 13.5 × 13.5 mm pixel size was mounted on the top of a dark chamber, and the animal was immobilized using isoflurane anesthesia. A specially designed lens system with 0.5 numerical aperture (on the detector side) and 7 pieces of the restricted number of lenses was used for the UPE measurement, leading 47 photon/s/cm^2 as a minimum detectable number of photons on each pixel. Using this equipment, UPE can be described by intensity (counts/15 min/pixel) at five independent regions on each paw, and was used for further correlation analysis. The regions were named according to the paw measured, and numbers were added (ranging from 1 to 5, indicating the location closest to the tip of the paw through the location farthest from the tip of the paw) as follows: LFP (left front paw) 1 through LFP5; LHP (left hind paw) 1 through LHP5; RFP (right front paw) 1 through RFP5; and RHP (right hind paw) 1 through RHP5.

2.2.2. Extraction of Plasma Metabolites and Metabolomics Analysis

Plasma samples were aliquoted and extracted via different methods in order to obtain separate classes of compounds, including oxylipins, amine metabolites, and oxidative stress–related metabolites. Oxylipins (bioactive lipid mediators derived from polyunsaturated fatty acids) were extracted using solid phase extraction and analyzed using an Agilent 1290 HPLC coupled to an Agilent 6490 triple quadrupole mass spectrometer with electrospray ionization as described previously [14,39]. Amine metabolites (including free amino acids and their biogenic metabolites) were extracted using AccQ-TagAQC derivatization and analyzed using a Waters ACQUITY UPLC coupled to a Waters Xevo mass spectrometer with electrospray ionization source as described by Noga et al. [40]. Oxidative stress–mediated metabolites—primarily PGs/IsoPGs, NO_2-FAs, lysophosphatidic acids, and sphingosine/sphingosine-related sphingolipids—were extracted using liquid–liquid extraction and analyzed using a validated method with an Agilent 1290 HPLC coupled to an Agilent 6490 triple quadrupole mass spectrometer with electrospray ionization. The peak area of each target compound was corrected using the appropriate internal standard (ISTD), leading to a ratio (target compound/ISTD) that was used for further analysis in the correlation study.

2.3. Data Preprocessing and Statistical Analysis

The metabolomics and UPE data collected from both the CIA and Ctrl groups were included in the correlation analysis. Univariate correlations were performed using the Spearman's rank correlation method using RStudio software (version 3.0.3). Absolute values of the Spearman's rank correlation coefficient ($|r|$) >0.7 were considered to reflect a strong correlation between parameters, and this threshold was used to create highly correlated graphical networks using Cytoscape software (version 3.3.0, http://www.cytoscape.org) with the MetScape plug-in for extracting and integrating information and for visualizing the correlation networks [41,42]. Positive and negative correlations were indicated by positive and negative values of *r*, respectively.

3. Results and Discussion

3.1. Collagen-induced Arthritis Alters the Local Distribution of UPE

Differences in UPE between CIA and Ctrl mice have been reported previously [20]. A schematic figure was displayed, in order to show the CCD setup of UPE instrument as well as the locations for UPE measurements on mouse front and hind paws (Fig. 1). Here, we used correlation networks to visualize the relationship between individual UPE

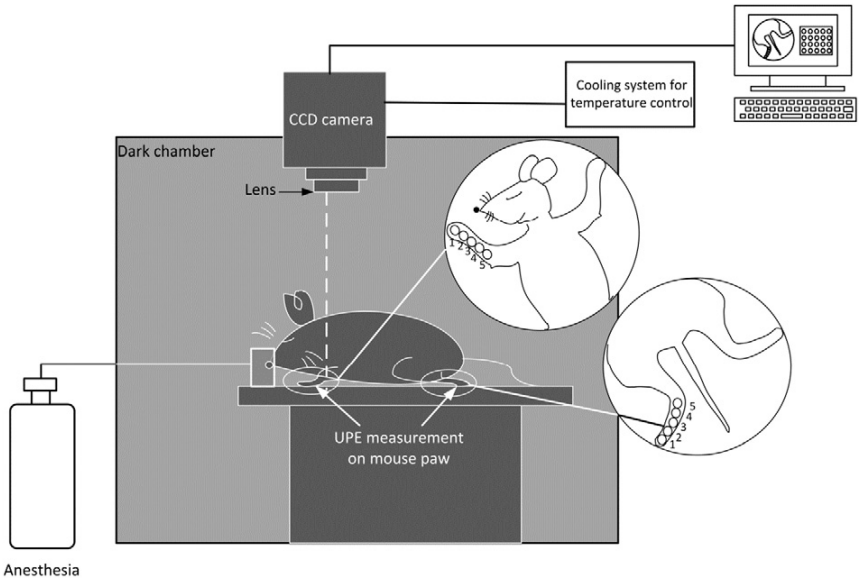

Fig. 1. Schematic figure of CCD set-up as well as locations for UPE measurements on mouse front and hind paws. Adapted from E. van Wijk et al. [20].

intensities at the locations measured in both CIA mice and in Ctrl mice (Fig. 2), as visualizing the profile of location-based UPE may provide important information regarding the disease. We then interpreted the differences and similarities between the two groups with respect to their correlation structures.

The correlations were quantified using the parameters (i.e., $|r|$ values and p-values) obtained from the Spearman correlation analysis. In total, 71 and 26 strongly positive UPE-to-UPE correlations were found in the CIA and Ctrl groups, respectively; no strongly negative correlations were found. The difference in the number of strongly positive correlations between the CIA and Ctrl groups can be seen visually in Fig. 2. In the CIA group, UPE intensity was tightly correlated between the two front paws and between the two hind paws (Fig. 2a). In contrast, we found no clear correlation patterns in the Ctrl group (Fig. 2b).

3.2. Differences in Metabolite Correlations Between CIA Mice and Control Mice

Next, we acquired metabolic data from plasma samples using HPLC-MS/MS (raw data are presented in Supplemental Table 2). The following three groups of metabolites were extracted using three validated methods and detected using three specific instruments: amine metabolites (including free amino acids and their biogenic metabolites), oxylipins, and oxidative stress–related metabolites. A total of 110 endogenous metabolites were detected in the plasma samples, including 30 oxylipins, 45 amine metabolites, and 35 oxidative stress–related lipids. Univariate and multivariate analyses were then applied to the metabolite sets in order to characterize the differences between CIA mice and Ctrl mice at the metabolomics level. Previously, we reported

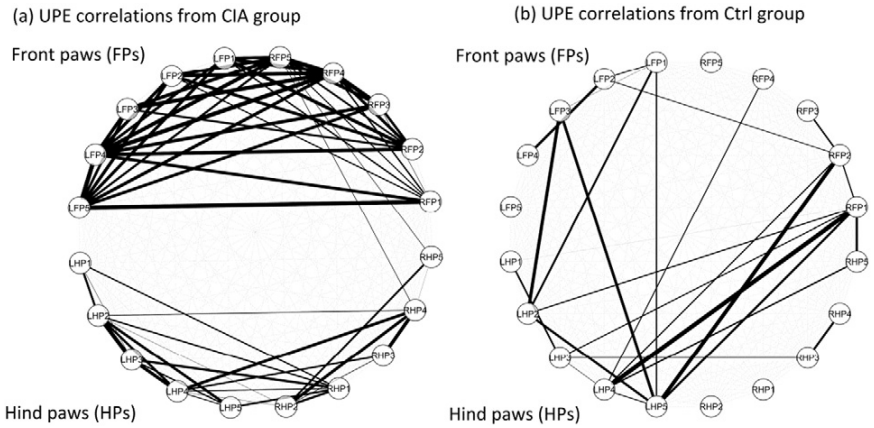

Fig. 2. Bio-photonic variance is revealed by location-based UPE-to-UPE correlation networks. The figure illustrates the differences in correlations between CIA mice (a) and Ctrl mice (b). In CIA mice, the strong correlations also indicate a strong similarity in UPE between the LFP (left front paw) and RFP (right front paw), as well as between the LHP (left hind paw) and RHP (right hind paw). The numbers (1 through 5) indicate the specific locations for the measurements (see Materials and Methods), (raw data are presented in Supplemental Table 1). Thus, the differences between the front paws and hind paws are clearly visible in the CIA group. The networks were established using the Spearman correlation analysis, and the lines represent Spearman correlation coefficients ($|r|$) >0.7.

Table 1
Summary of the key metabolites that differed significantly between the CIA and Ctrl groups.

Oxylipins		Amine metabolites		Oxidative stress	
Compound	Changes	Compound	Changes	Compound	Changes
9,10-DiHOME	↓	Methionine	↓	PGE3	↓
9-KODE	↓	Homocysteine	↓	8,12-iso-iPF2a	↓
13-HDoHE	↑	Threonine	↓	cyclic-LPA C16:0	↓
14-HDoHE	↑	Proline	↓	cyclic-LPA C18:2	↓
12,13-DiHOME	↓	Alanine	↓		
9,12,13-TriHOME	↓	Valine	↓		
12-HEPE	↑	Cystathionine	↓		
9,10,13-TriHOME	↓	Lysine	↓		
9,10-EpOME	↓	Glycylglycine	↓		
10-HDoHE	↑	Serine	↓		
9-HODE[a]	↓	Asparagine	↓		
8-HETE[a]	↑	Cysteine	↓		
13-KODE[a]	↓	Tryptophan	↓		
12,13-EpOME[a]	↓	Methionine sulfoxide	↓		
13,14-dihydro-PGF2a[a]	↑	Homocitrulline	↓		
12-HETE[a]	↑	Isoleucine	↓		
		Gamma-glutamylalanine	↓		
		Histidine	↓		
		Glutamine	↓		
		Leucine	↓		

Abbreviations: DiHOME, dihydroxyoctadeca(mono)enoic acid; EpOME, epoxyoctadecamonoenoic acid; HDoHE, hydroxydocosahexaenoic acid; HEPE, hydroxyeicosapentaenoic acid; HETE, hydroxyeicosatetraenoic acid; HODE, hydroxyoctadecadienoic acid; KODE, ketooctadecadienoic acid; PG, prostaglandin; TriHOME, trihydroxyoctadecenoic acid.
↓: Decreased in CIA mice; ↑: Increased in CIA mice.
[a] Extra important oxylipins which contributed to the group clustering are based on multivariate analysis (VIP > 1).

the differences between CIA mice and Ctrl mice with respect to oxylipins and amine metabolites [14,19]. Based on the oxidative stress platform, after log transformation and auto-scaling of the data, we also found a number of key metabolites that differed between the CIA the Ctrl groups ($p < 0.05$, Student's t-test). Table 1 summarizes the key metabolites that differed significantly between the CIA and Ctrl groups.

Differences in metabolites generally do not occur independently, but often change together with other, related metabolites, as metabolic reactions are often part of a dynamic system and have many biological processes in common [35]. Metabolic network analysis is an emerging approach used to diagnose disease, and it has the advantage of integrating "omics" datasets in order to identify links and select useful information from among chaos [34,43]. We therefore performed a correlation network analysis in order to visualize pair-wise metabolic correlations and to extract novel information regarding dynamic alternatives. A merge between the metabolite-to-metabolite correlation networks measured in the plasma of CIA and Ctrl mice is illustrated in Fig. 3a and b, respectively. Next, the Spearman correlation coefficient between metabolites (r_m) was calculated, and only strong correlations (either positive or negative) (i.e., with an $|r_{m.}|$ value >0.7) were included in the resulting network. We found a total of 394 positive correlations and 91 negative correlations in the CIA group, and a total of 864 positive correlations and 117 negative correlations in the Ctrl group (raw data of correlation results see Supplemental Table 3). In general, metabolites that are in the same chemical class or in the same biochemical pathway tended to correlate with each other; these so-called "chemical class-based" clusters and "pathway-based" clusters were more pronounced in the Ctrl group, leading a highly connected region among oxylipins and another region among amine metabolites. This network analysis revealed certain structural or pathway similarities among those highly connected metabolites with respect to significant positive correlations. Moreover, the associations between oxylipins and amine metabolites were relatively weak in the Ctrl group, possible because oxylipins and amine metabolites are generated via two separate metabolic pathways.

Interestingly, we found that some of the strong correlations in the Ctrl group—including both "oxylipin-to-oxylipin" and "amine-to-amine" correlations—were weaker in the CIA group. In contrast, the CIA group contained more negative oxylipin-to-amine correlations (Fig. 3a) than the Ctrl group (Fig. 3b). For example, the HETEs and HDoHEs that were elevated in CIA mice were strongly correlated with the branched chain amino acids valine, leucine, and isoleucine, as well as with cystathionine, alanine, glutamine, and asparagine. The use of HETEs and HDoHEs as inflammatory/ROS-related biomarkers has been described previously [14], and we also found that decreases in these amine metabolites may reflect muscle wasting and/or energy expenditure (cachexia) in RA [19]. Therefore, our analysis of metabolic correlation networks suggests that the increased inflammation and ROS levels reflected by oxylipins may also be associated with the onset of muscle wasting and increased energy expenditure in RA.

3.3. UPE Is Correlated With Inflammatory Signaling-related Metabolites in CIA Mice

As discussed in the Introduction, UPE arises as a result of metabolic reactions, particularly oxidation-reduction (redox) reactions; therefore, we hypothesized that UPE emission patterns may be correlated with metabolite patterns. To test this hypothesis, we created a correlation network to visualize potential associations between UPE intensity and peak area ratios of measured metabolites (see Materials and Methods). Therefore, we used UPE-to-metabolite correlations (i.e., between a given UPE value, u, and a given metabolite, m) in the correlation networks, and the Spearman correlation coefficient $|r_{um}|$ was calculated for each UPE-metabolite pair in both the CIA group and the Ctrl group.

The heat map in Fig. 4 depicts a general UPE-to-metabolite correlation profile used to compare the differences measured between the CIA group and the Ctrl group (data see in Supplemental Table 4). A cluster analysis reveals clear location-based clusters in the CIA mice. The heat map also indicates a systemic change in the CIA group (i.e., the majority of positive correlations, shown in red) compared with the Ctrl group (i.e., the majority of negative correlations, shown in green). After removing relative weaker coefficient from the Spearman correlation analysis ($|r_{um}| < 0.7$), networks were built to reflect the highly correlated entities and to show the most important metabolites (Fig. 4b). After we removed the relatively weaker correlations from the Spearman correlation analysis (i.e., $|r_{um}|$ values <0.7), we built a network to reflect the strongly correlated entities and to illustrate the most relevant metabolites (Fig. 4b). Circle-attributed networks were then used to identify the key correlations and to compare the CIA group with the Ctrl group. A

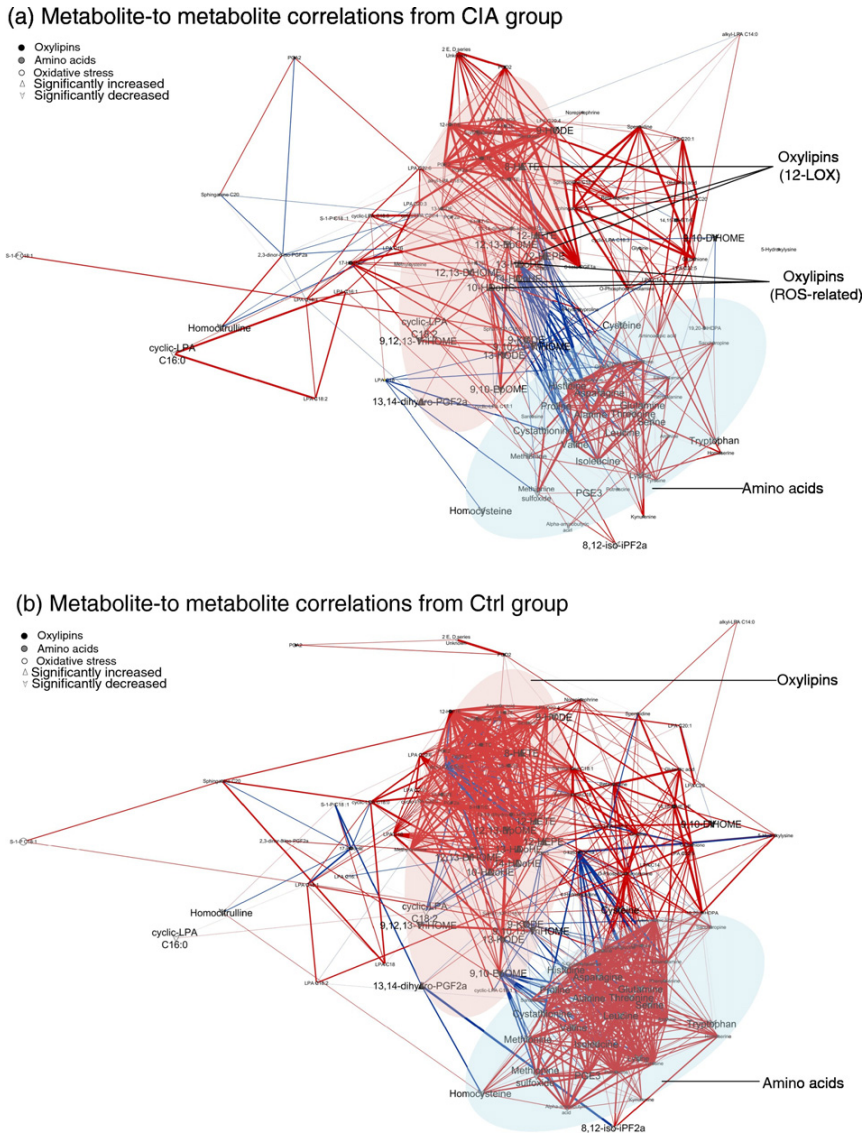

Fig. 3. Metabolic correlation networks in the CIA and Ctrl groups. Depicted are the metabolite-to-metabolite correlation networks for CIA (3a) and Ctrl (3b) mice. All of the metabolites detected in our analysis are included in the networks models. Nodes with a positive correlation are indicated with solid red lines, and nodes with a negative correlation are indicated by solid blue lines. Shaded ellipses with a light red or light blue background indicate clusters of oxylipins or amine metabolites, respectively. Thickness of lines indicate gradient correlation strength: the thicker the line is, the stronger the correlation is (visible correlation co-efficiency: $|r|$ ranges from 0.7 to 1).

total of 27 strongly positive correlations and 79 negative correlations were identified in the Ctrl group, and a total of 146 positive and 9 negative correlations were identified in the CIA group.

The correlation networks revealed that the majority of UPE-to-metabolite correlations in the Ctrl group were negative, whereas the majority of UPE-to-metabolite correlations in the CIA group were strongly positive. The major metabolites that were positively correlated with UPE in the CIA group are the monohydroxyeicosatetraenoic acids (HETEs), prostaglandins (PGs), thromboxane (TBX) synthase products, lysophosphatidic acids (LPAs), sphingolipid signaling molecules, and some amine metabolites (Fig. 4b). UPE intensity measured at various locations was correlated with various metabolites in the CIA group. For example, UPE intensity in the front paws was more strongly correlated with some LPAs, whereas UPE intensity in the hind paws was more strongly correlated with PGs (13,14-dihydro-15-keto-PGF2a, PGE_2, PGD_2, and 6-keto-PGF2a), TBX synthase products (TBX2 and 12-HHTrE), HETEs (8-HETE, 15-HETE, 11-HETE, and 12-HETE), and sphingolipids; see the CIA correlation networks in Fig. 4b.

Next, the pathways related to these metabolites based on our previous study [14] and the Kyoto Encyclopedia of Genes and Genomes were organized (Fig. 5). LPAs act on G protein–coupled signaling and cellular signaling responses and function as inflammatory mediators [44,45]. PGs and TBXs, which are synthesized from arachidonic acid via COX-II pathways, have well-established pro-inflammatory functions [46,47]. The 12/15-LOX products (12-HETE, 15-HETE, and 8-HETE) promote the production of cytokines and activate the NF-κB pathway to inhibit cellular apoptosis [48,49]. In addition, 8-HETE, 12-HETE, and 11-HETE can also be peroxided non-enzymatically by ROS to inhibit apoptosis [50–54]; therefore, these three HETEs may be important inflammatory mediators [55,56]. The sphingomyelin-derived sphingolipids sphingosine and sphingosine-1-phosphate (S1P) are signaling molecules in immune cells that mediate neutrophil activation and apoptosis, and are

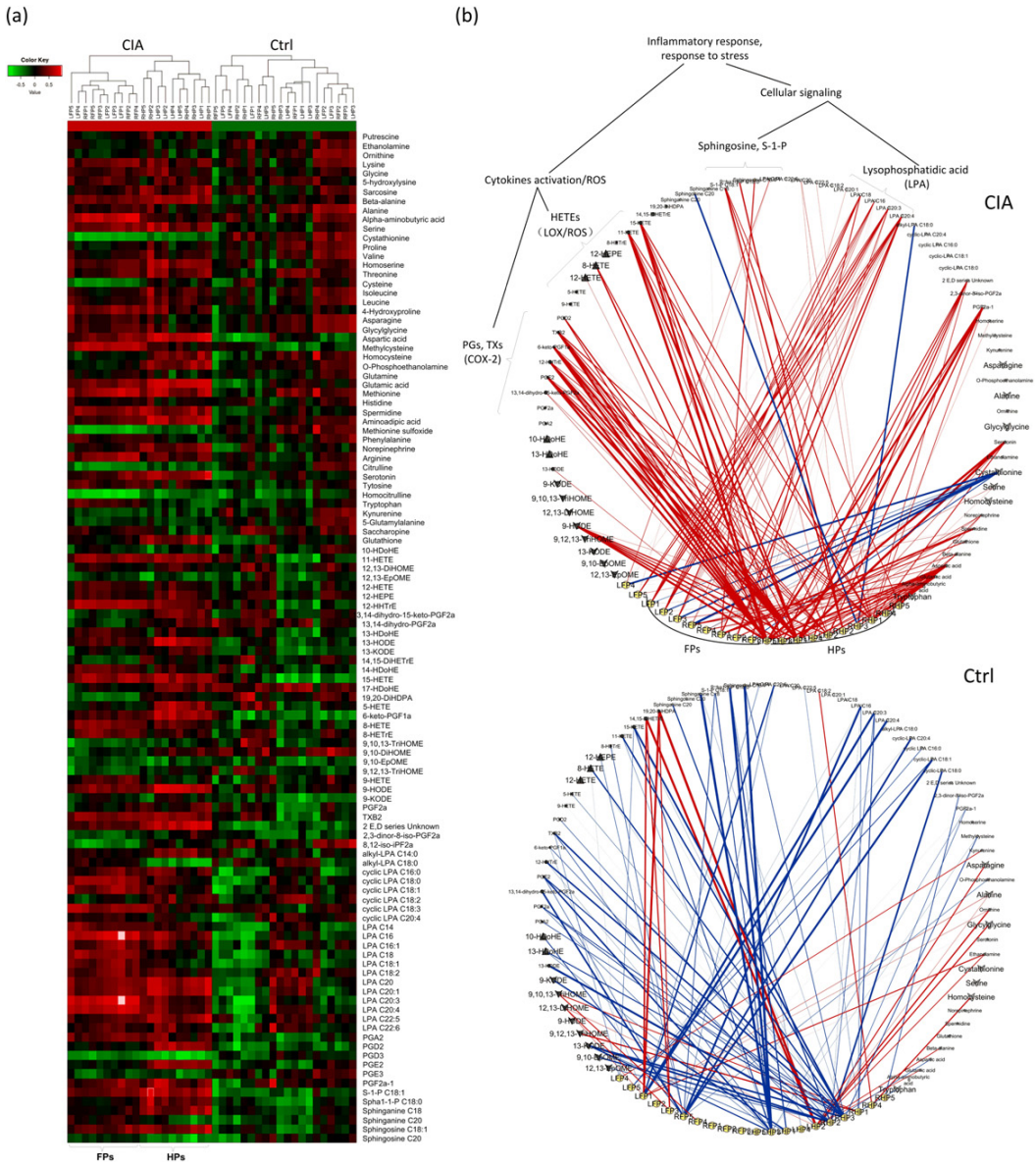

Fig. 4. Correlation-based analysis between UPE and metabolites measured in the plasma of CIA mice and Ctrl mice. a) Heat map showing the entire UPE-metabolite correlation profile, as well as the differences between the CIA and Ctrl mice. Colored blocks represent the value of the correlation coefficient, which were color-coded from 1 (strongly positive, light red) to −1 (strongly negative, light green). b) Visualized network model of the strong correlations (defined as a $|r_{um}|$ value >0.7). Several important pathway-related networks reflect the inflammation, ROS production, and muscle wasting associated with RA. Each dot indicates an individual parameter that includes a given metabolite and UPE value: yellow dots reflect location-based UPE intensity, and black, gray, and white dots represent oxylipins, biogenic amines, and oxidative stress–related metabolites, respectively. Also shown (between the Ctrl and CIA network models) are enlarged views of the key metabolites that differed significantly based on our univariate and multivariate analyses. The up-triangles and down-triangles indicate the direction of the metabolic change in the CIA mice (i.e., up-regulation or down-regulation, respectively). The red and blue lines indicate positive and negative correlations, respectively, and the thickness of the lines indicate the strength of the correlation.

therefore also considered to be inflammatory mediators [57–62]. Based on the correlation networks, it can be seen that these inflammatory mediators participated in the systemic perturbations (measured using both metabolomics and UPE) in the CIA mice, even though some of these mediators were not altered significantly in our univariate analysis. We also conclude that UPE intensity is correlated with systemic inflammatory mediators, ROS mediators, and cellular signaling processes; therefore, measuring UPE intensity may provide a means to diagnose inflammatory disease. In addition, UPE may also be used to monitor lipid peroxidation which relate to inflammation and ROS level in both healthy and diseased individuals (Fig. 6). Thus, a specific phenotype of a disease can be complemented by measuring both "omics" profiles and UPE patterns, thereby providing a more detailed understanding of the disease and its underlying processes.

In the CIA mice, a strongly negative correlation between cystathionine and UPE was measured, whereas several amine metabolites—including serotonin, tryptophan, and aspartic acid—were positively correlated with UPE. Cystathionine is a scavenger of free radicals [63]; therefore, given its significant decrease in CIA mice compared to Ctrl mice, the negative correlation between cystathionine and UPE intensity indicates that the increase in UPE intensity may be due to a decrease in antioxidants in RA. Both tryptophan metabolism and the

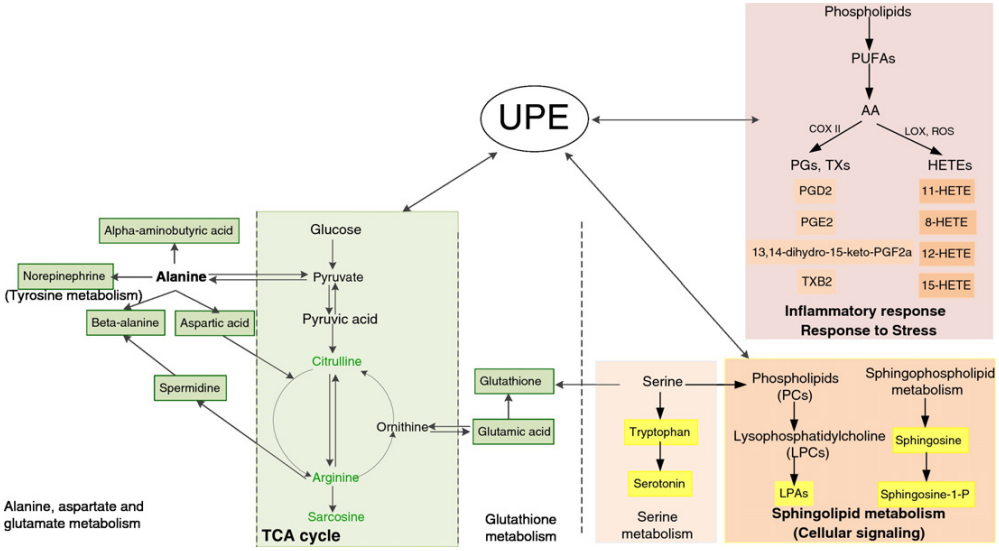

Fig. 5. Putative biochemical pathways with metabolites that can be correlated with UPE. UPE intensity can be linked to inflammatory responses and ROS-related stress in RA, which are reflected by COX-II and 12/15-LOX oxylipins derived from arachidonic acid (AA). During cell signaling, the production of LPAs and sphingosine also associates with the increased UPE intensity. Another pathway that may be linked with UPE intensity is the TCA cycle.

serotonergic system have been well described as key pathways that can influence signaling in the central nervous system [64]. Thus, UPE may also be correlated with metabolic systems that are associated with neurotransmission. In addition, based upon pathways that regulate amine metabolites listed in the Kyoto Encyclopedia of Genes and Genomes, all of the other amine metabolites that were positively correlated with UPE are associated either directly or indirectly with the TCA cycle (see Fig. 5). The correlations identified between UPE intensity and these metabolites may suggest that during disease, some of the electrons that would otherwise participate in chemical reactions to produce energy (for example, with amine metabolites in the TCA cycle) actually escape and set free the energy which they carry, as photons, whereby the electrons change from high to low energy level states. Simultaneously, free radicals and/or ROS are produced, driving lipid peroxidation to produce inflammatory HETEs and PGs. While such a speculation need more rigorous validation.

The reduction in amine metabolites in the plasma of CIA mice compared to Ctrl mice may be linked to the contribution of muscle wasting in arthritis [19]. Considering that we found strong correlations between amine metabolites and UPE intensity, and given that muscle wasting is a common feature in many disease processes, including some cancers [65], HIV/AIDs [66], type 2 diabetes [67], renal failure, uremia [68], and heart failure [69], UPE may also have potential perspective for the use of monitoring energy wasting and muscle wasting in other diseases. In

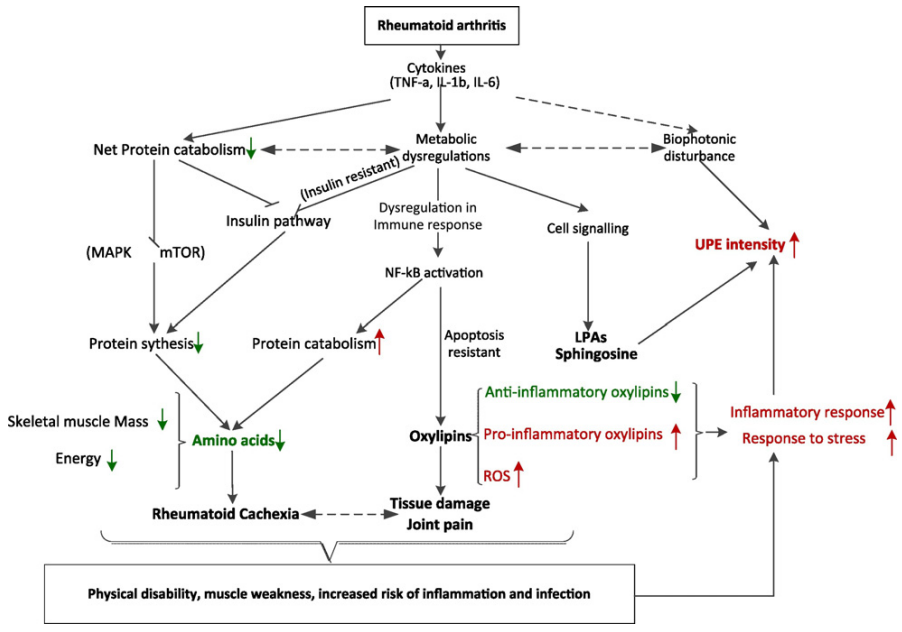

Fig. 6. Systemic and dynamic changes in RA. The production of cytokines dynamically interrupts living systems at both the biochemical level (i.e., the proteomics and metabolomics levels) and the bio-photon level. In addition, the biochemical changes are in correlation to the UPE changes. Elements marked in red/green are those increased/decreased in our CIA mice model.

this respect, future studies should examine the relationship between muscle wasting and UPE.

Interestingly, HETEs, PGs, sphingosine, and S1P—which were strongly correlated with UPE intensity in our study—are also considered to be important inflammatory biomarkers in a variety of diseases, including RA [70], cardiovascular disease and/or atherosclerosis–related inflammation [59,61,71–72], congestive heart failure [60], cancers and other tumors [54,73], some prostate diseases [55], and nonalcoholic steatohepatitis [56]. Therefore, our finding that UPE is correlated with these inflammatory mediators may shed light on the biological mechanisms that underlie these diseases from a systems biology perspective.

4. Conclusions

Given its complex pathophysiology, RA has been studied using a variety of technologies and approaches. Indeed, integrating various data sets can provide important information regarding the disease process and possible treatment strategies. Generating correlation networks can provide valuable information, and these networks have been used recently within a wide range of "omics" studies, including proteomics, genomics, and metabolomics, thereby helping distinguish specific diseases and/or phenotypes [34–35,74]. Here, we performed the first study that integrates UPE with metabolomics in both diseased mice (i.e., mice with collagen-induced arthritis) and healthy control mice; this novel, powerful approach yielded meaningful information regarding RA. Moreover, we found specific correlations between metabolomics and UPE. Lastly, our correlation network analysis shows a systematic way to illustrate the complexity of RA, including dysregulation of both UPE and metabolomics.

Using our correlation networks, we also found that oxylipins were negatively correlated with certain amine metabolites in the CIA group. This may indicate a systematic perturbation under inflammation and ROS response in RA-induced situation. However, further study is needed in order to elucidate whether the inflammation and ROS are the consequence of muscle wasting, or vice versa. We also found that UPE was correlated with certain inflammatory mediators, and we expanded the biological interpretation of RA using correlation networks.

In conclusion, our correlation network analysis provides valuable information regarding the disease process from a system-wide perspective. Understanding the underlying biochemical phenomena that give rise to UPE is of great importance to learn about potential applications of UPE in early disease characterization.

Acknowledgments

Min He was supported by the Chinese Scholarship Council (Scholarship File Number 20108220166) and 973 Program (No. 2014CB543100). Additional support was provided by the Samueli Institute in Alexandria, VA. The authors are grateful to Prof. Masaki Kobayashi at the Tohoku Institute of Technology in Sendai, Japan for providing the use of laboratory facilities and for collecting plasma samples. We are also grateful to Johannes C. Schoeman for support preparing the oxidative stress samples and for help with data processing.

Appendix A. Supplementary Data

Supplementary data to this article can be found online at http://dx.doi.org/10.1016/j.jphotobiol.2016.12.036.

References

[1] Y. Alamanos, A. Drosos, Epidemiology of adult rheumatoid arthritis, Autoimmun. Rev. 4 (3) (2005) 130–136.
[2] S.E. Gabriel, The epidemiology of rheumatoid arthritis, Rheum. Dis. Clin. N. Am. 27 (2) (2001) 269–281.
[3] G.S. Firestein, Evolving concepts of rheumatoid arthritis, Nature 423 (6937) (May 2003) 356–361.
[4] E.H. Choy, G.S. Panayi, Cytokine pathways and joint inflammation in rheumatoid arthritis, N. Engl. J. Med. 344 (12) (Mar. 2001) 907–916.
[5] G. Ferraccioli, L. Bracci-Laudiero, S. Alivernini, E. Gremese, B. Tolusso, F. De Benedetti, Interleukin-1β and interleukin-6 in arthritis animal models: roles in the early phase of transition from acute to chronic inflammation and relevance for human rheumatoid arthritis, Mol. Med. 16 (11–12) (2010) 552–557.
[6] S.S. Makarov, NF-kappa B in rheumatoid arthritis: a pivotal regulator of inflammation, hyperplasia, and tissue destruction, Arthritis Res. 3 (4) (2001) 200–206.
[7] R. Holmdahl, R. Bockermann, J. Bäcklund, H. Yamada, The molecular pathogenesis of collagen-induced arthritis in mice—a model for rheumatoid arthritis, Ageing Res. Rev. 1 (1) (Feb. 2002) 135–147.
[8] A.-K.B. Lindqvist, R. Bockermann, Å.C.M. Johansson, K.S. Nandakumar, M. Johannesson, R. Holmdahl, Mouse models for rheumatoid arthritis, Trends Genet. 18 (6) (Jun. 2002) S7–S13.
[9] K.S. Nandakumar, R. Holmdahl, Efficient promotion of collagen antibody induced arthritis (CAIA) using four monoclonal antibodies specific for the major epitopes recognized in both collagen induced arthritis and rheumatoid arthritis, J. Immunol. Methods 304 (1–2) (Sep. 2005) 126–136.
[10] D.D. Brand, K.A. Latham, E.F. Rosloniec, Collagen-induced arthritis, Nat. Protoc. 2 (5) (2007) 1269–1275.
[11] J. Eguchi, T. Koshino, T. Takagi, T. Hayashi, T. Saito, NF-kappa B and I-kappa B overexpression in articular chondrocytes with progression of type II collagen-induced arthritis in DBA/1 mouse knees, Clin. Exp. Rheumatol. 20 (5) (2002) 647–652.
[12] R. Ramautar, R. Berger, J. van der Greef, T. Hankemeier, Human metabolomics: strategies to understand biology, Curr. Opin. Chem. Biol. 17 (5) (2013) 841–846.
[13] H. Van Wietmarschen, J. Van Der Greef, Metabolite space of rheumatoid arthritis, Br. J. Med. Med. Res. 2 (3) (2012) 469–483.
[14] M. He, E. Van Wijk, R. Berger, M. Wang, K. Strassburg, C. Schoeman, R.J. Vreeken, H. Van Wietmarschen, A.C. Harms, T. Hankemeier, J. Van Der Greef, Collagen induced arthritis in DBA/1J mice associates with oxylipin changes in plasma, Mediat. Inflamm. 2015 (2015) 1–11.
[15] J. Walsmith, R. Roubenoff, Cachexia in rheumatoid arthritis, Int. J. Cardiol. 85 (1) (2002) 89–99.
[16] R. Roubenoff, Sarcopenic obesity: does muscle loss cause fat gain? Lessons from rheumatoid arthritis and osteoarthritis, Ann. N. Y. Acad. Sci. 904 (May 2000) 553–557.
[17] O.M. da Rocha, A.D.A.P. Batista, N. Maestá, R.C. Burini, I.M.M. Laurindo, Sarcopenia in rheumatoid cachexia: definition, mechanisms, clinical consequences and potential therapies, Rev. Bras. Reumatol. 49 (3) (2009) 294–301.
[18] G.D. Summers, C.M. Deighton, M.J. Rennie, A.H. Booth, Rheumatoid cachexia: a clinical perspective, Rheumatology 47 (8) (2008) 1124–1131.
[19] M. He, A.C. Harms, E. van Wijk, M. Wang, R. Berger, S. Koval, T. Hankemeier, J. van der Greef, The role of amino acids in rheumatoid arthritis studied by metabolomics, Int. J. Rheum. Dis. (2017) http://dx.doi.org/10.1111/1756-185X.13062.
[20] E. van Wijk, M. Kobayashi, R. van Wijk, J. van der Greef, Imaging of ultra-weak photon emission in a rheumatoid arthritis mouse model, PLoS One 8 (12) (Jan 2013), e84579. .
[21] M. Cifra, P. Pospíšil, Ultra-weak photon emission from biological samples: definition, mechanisms, properties, detection and applications, J. Photochem. Photobiol. B Biol. 139 (Oct. 2014) 2–10.
[22] M. Kobayashi, M. Takeda, T. Sato, Y. Yamazaki, K. Kaneko, K. Ito, H. Kato, H. Inaba, In vivo imaging of spontaneous ultraweak photon emission from a rat's brain correlated with cerebral energy metabolism and oxidative stress, Neurosci. Res. 34 (2) (Jul. 1999) 103–113.
[23] R. Van Wijk, E. Van Wijk, F. Wiegant, J. Ives, Free radicals and low-level photon emission in human pathogenesis: state of the art, Indian J. Exp. Biol. 46 (5) (May 2008) 273–309.
[24] R. Van Wijk, E. Van Wijk, H. van Wietmarschen, J. Van der Greef, Towards whole-body ultra-weak photon counting and imaging with a focus on human beings: a review, J. Photochem. Photobiol. B Biol. 139 (Oct. 2014) 39–46.
[25] A. Rastogi, P. Pospísil, Spontaneous ultraweak photon emission imaging of oxidative metabolic processes in human skin: effect of molecular oxygen and antioxidant defense system, J. Biomed. Opt. 16 (9) (2011) 96005.
[26] P. Pospíšil, A. Prasad, M. Rác, Role of reactive oxygen species in ultra-weak photon emission in biological systems, J. Photochem. Photobiol. B Biol. 139 (Oct. 2014) 11–23.
[27] A. Prasad, P. Pospíšil, Linoleic acid-induced ultra-weak photon emission from *Chlamydomonas reinhardtii* as a tool for monitoring of lipid peroxidation in the cell membranes, PLoS One 6 (7) (Jan 2011), e22345. .
[28] J.A. Ives, E. van Wijk, N. Bat, C. Crawford, A. Walter, W.B. Jonas, R. van Wijk, J. van der Greef, Ultraweak photon emission as a non-invasive health assessment: a systematic review, PLoS One 9 (2) (Feb. 2014), e87401. .
[29] M. He, M. Sun, E. van Wijk, H. van Wietmarschen, R. van Wijk, Z. Wang, M. Wang, T. Hankemeier, J. van der Greef, A Chinese literature overview on ultra-weak photon emission as promising technology for studying system-based diagnostics, Complement. Ther. Med. 25 (2016) 20–26.
[30] A. Rastogi, P. Pospísil, Spontaneous ultraweak photon emission imaging of oxidative metabolic processes in human skin: effect of molecular oxygen and antioxidant defense system, J. Biomed. Opt. 16 (9) (Sep. 2011) 96005.
[31] C. de Mello Gallep, Ultraweak, spontaneous photon emission in seedlings: toxicological and chronobiological applications, Luminescence 29 (8) (Dec. 2014) 963–968.
[32] S.E. Calvano, W. Xiao, D.R. Richards, R.M. Felciano, H.V. Baker, R.J. Cho, R.O. Chen, B.H. Brownstein, J.P. Cobb, S.K. Tschoeke, C. Miller-Graziano, L.L. Moldawer, M.N. Mindrinos, R.W. Davis, R.G. Tompkins, S.F. Lowry, A network-based analysis of systemic inflammation in humans, Nature 437 (7061) (Oct. 2005) 1032–1037.

[33] A.-L. Barabasi, N. Gulbahce, J. Loscalzo, Network medicine: a network-based approach to human disease, Nat. Rev. Genet. 12 (1) (2011) 56–68.
[34] Y. Noguchi, N. Shikata, Characterization of dietary protein-dependent amino acid metabolism by linking free amino acids with transcriptional profiles through analysis of correlation, Physiology 34 (3) (2008) 315–326.
[35] K. Morgenthal, W. Weckwerth, R. Steuer, Metabolomic networks in plants: transitions from pattern recognition to biological interpretation, Biosystems 83 (2–3) (2006) 108–117.
[36] J. van der Greef, S. Martin, P. Juhasz, A. Adourian, T. Plasterer, E.R. Verheij, R.N. McBurney, The art and practice of systems biology in medicine: mapping patterns of relationships, J. Proteome Res. 6 (4) (Apr. 2007) 1540–1559.
[37] C.A. Hidalgo, N. Blumm, A.-L. Barabási, N.A. Christakis, A dynamic network approach for the study of human phenotypes, PLoS Comput. Biol. 5 (4) (Apr. 2009), e1000353. .
[38] S. Yoshino, E. Sasatomi, M. Ohsawa, Bacterial lipopolysaccharide acts as an adjuvant to induce autoimmune arthritis in mice, Immunology 99 (4) (Apr. 2000) 607–614.
[39] K. Strassburg, A.M.L. Huijbrechts, K.A. Kortekaas, J.H. Lindeman, T.L. Pedersen, A. Dane, R. Berger, A. Brenkman, T. Hankemeier, J. van Duynhoven, E. Kalkhoven, J.W. Newman, R.J. Vreeken, Quantitative profiling of oxylipins through comprehensive LC-MS/MS analysis: application in cardiac surgery, Anal. Bioanal. Chem. 404 (5) (Sep. 2012) 1413–1426.
[40] M.J. Noga, A. Dane, S. Shi, A. Attali, H. van Aken, E. Suidgeest, T. Tuinstra, B. Muilwijk, L. Coulier, T. Luider, T.H. Reijmers, R.J. Vreeken, T. Hankemeier, Metabolomics of cerebrospinal fluid reveals changes in the central nervous system metabolism in a rat model of multiple sclerosis, Metabolomics 8 (2) (Apr. 2012) 253–263.
[41] P. Shannon, A. Markiel, O. Ozier, N.S. Baliga, J.T. Wang, D. Ramage, N. Amin, B. Schwikowski, T. Ideker, Cytoscape: a software environment for integrated models of biomolecular interaction networks, Genome Res. 13 (11) (Nov. 2003) 2498–2504.
[42] J. Gao, V.G. Tarcea, A. Karnovsky, B.R. Mirel, T.E. Weymouth, C.W. Beecher, J.D. Cavalcoli, B.D. Athey, G.S. Omenn, C.F. Burant, H.V. Jagadish, Metscape: acytoscape plug-in for visualizing and interpreting metabolomic data in the context of human metabolic networks, Bioinformatics 26 (7) (2010) 971–973.
[43] T. Kimura, Y. Noguchi, N. Shikata, M. Takahashi, Plasma amino acid analysis for diagnosis and amino acid-based metabolic networks, Curr. Opin. Clin. Nutr. Metab. Care 12 (1) (Jan. 2009) 49–53.
[44] W.H. Moolenaar, O. Kranenburg, F.R. Postma, G.C.M. Zondag, Lysophosphatidic acid: G-protein signalling and cellular responses, Curr. Opin. Cell Biol. 9 (2) (1997) 168–173.
[45] C. Zhao, M.J. Fernandes, G.D. Prestwich, J. Di Battista, T. Clair, P.E. Poubelle, S.G. Bourgoin, Regulation of lysophosphatidic acid receptor expression and function in human synoviocytes : implications for rheumatoid arthritis ? Mol. Pharmacol. 73 (2) (2008) 587–600.
[46] K. Takayama, K. Yuhki, K. Ono, T. Fujino, A. Hara, T. Yamada, S. Kuriyama, H. Karibe, Y. Okada, O. Takahata, T. Taniguchi, T. Iijima, H. Iwasaki, S. Narumiya, F. Ushikubi, Thromboxane A2 and prostaglandin F2alpha mediate inflammatory tachycardia, Nat. Med. 11 (5) (2005) 562–566.
[47] N. Sugino, A. Karube-Harada, T. Taketani, A. Sakata, Y. Nakamura, Withdrawal of ovarian steroids stimulates prostaglandin F2alpha production through nuclear factor-kappaB activation via oxygen radicals in human endometrial stromal cells: potential relevance to menstruation, J. Reprod. Dev. 50 (2) (2004) 215–225.
[48] S.K. Chakrabarti, B.K. Cole, Y. Wen, S.R. Keller, L. Nadler, 12/15-Lipoxygenase products induce inflammation and impair insulin signaling in 3T3-L1 adipocytes, Obesity 17 (9) (2009) 1657–1663.
[49] M. Kandouz, D. Nie, G.P. Pidgeon, S. Krishnamoorthy, K.R. Maddipati, K.V. Honn, Platelet-type 12-lipoxygenase activates NF-kB in prostate cancer cells, Prostaglandins Other Lipid Mediat. 71 (3–4) (2003) 189–204.
[50] S.J. Muga, P. Thuillier, A. Pavone, J.E. Rundhaug, W.E. Boeglin, M. Jisaka, A.R. Brash, S.M. Fischer, 8S-lipoxygenase products activate peroxisome proliferator-activated receptor alpha and induce differentiation in murine keratinocytes, Cell Growth Differ. 11 (8) (Aug. 2000) 447–454.
[51] R.A. Daynes, D.C. Jones, Emerging roles of PPARs in inflammation and immunity, Nat. Rev. Immunol. 2 (10) (Oct. 2002) 748–759.
[52] H. Kühn, V.B. O'Donnell, Inflammation and immune regulation by 12/15-lipoxygenases, Prog. Lipid Res. 45 (4) (2006) 334–356.
[53] M.H. Shishehbor, R. Zhang, H. Medina, M.-L. Brennan, D.M. Brennan, S.G. Ellis, E.J. Topol, S.L. Hazen, Systemic elevations of free radical oxidation products of arachidonic acid are associated with angiographic evidence of coronary artery disease, Free Radic. Biol. Med. 41 (11) (Dec. 2006) 1678–1683.
[54] G.P. Pidgeon, J. Lysaght, S. Krishnamoorthy, J.V. Reynolds, K. O'Byrne, D. Nie, K.V. Honn, Lipoxygenase metabolism: roles in tumor progression and survival, Cancer Metastasis Rev. 26 (3–4) (Dec. 2007) 503–524.
[55] K. Nithipatikom, M.A. Isbell, W.A. See, W.B. Campbell, Elevated 12- and 20-hydroxyeicosatetraenoic acid in urine of patients with prostatic diseases, Cancer Lett. 233 (2) (2006) 219–225.
[56] P. Puri, M.M. Wiest, O. Cheung, F. Mirshahi, C. Sargeant, H.-K. Min, M.J. Contos, R.K. Sterling, M. Fuchs, H. Zhou, S.M. Watkins, A.J. Sanyal, The plasma lipidomic signature of nonalcoholic steatohepatitis, Hepatology 50 (6) (Dec. 2009) 1827–1838.
[57] M. Maceyka, S.G. Payne, S. Milstien, S. Spiegel, Sphingosine kinase, sphingosine-1-phosphate, and apoptosis, Biochim. Biophys. Acta Mol. Cell Biol. Lipids 1585 (2–3) (Dec. 2002) 193–201.
[58] Q. Liu, H. Rehman, Y. Shi, Y. Krishnasamy, J.J. Lemasters, C.D. Smith, Z. Zhong, Inhibition of sphingosine kinase-2 suppresses inflammation and attenuates graft injury after liver transplantation in rats, PLoS One 7 (7) (2012) e41834.
[59] F. Roviezzo, V. Brancaleone, L. De Gruttola, V. Vellecco, M. Bucci, B. D'Agostino, D. Cooper, R. Sorrentino, M. Perretti, G. Cirino, Sphingosine-1-phosphate modulates vascular permeability and cell recruitment in acute inflammation in vivo, J. Pharmacol. Exp. Ther. 337 (3) (Jun. 2011) 830–837.
[60] L. Dalla Libera, R. Sabbadini, C. Renken, B. Ravara, M. Sandri, R. Betto, A. Angelini, G. Vescovo, Apoptosis in the skeletal muscle of rats with heart failure is associated with increased serum levels of TNF-α and sphingosine, J. Mol. Cell. Cardiol. 33 (10) (2001) 1871–1878.
[61] S. Mahajan-Thakur, A. Böhm, G. Jedlitschky, K. Schrör, B.H. Rauch, Sphingosine-1-phosphate and its receptors: a mutual link between blood coagulation and inflammation, Mediat. Inflamm. 2015 (2015) 1–11.
[62] E.J. Goetzl, Y. Kong, B. Mei, Lysophosphatidic acid and sphingosine 1-phosphate protection of T cells from apoptosis in association with suppression of Bax, J. Immunol. 162 (4) (Feb. 1999) 2049–2056.
[63] K. Wada, Y. Kamisaki, K. Nakamoto, T. Itoh, Effect of cystathionine as a scavenger of superoxide generated from human leukocytes or derived from xanthine oxidase in vitro, Eur. J. Pharmacol. 296 (3) (1996) 335–340.
[64] J.P. Ruddick, A.K. Evans, D.J. Nutt, S.L. Lightman, G.A. Rook, C.A. Lowry, Tryptophan metabolism in the central nervous system: medical implications, Expert Rev. Mol. Med. 8 (20) (2006) 1–27.
[65] T.M. O'Connell, F. Ardeshirpour, S.A. Asher, J.H. Winnike, X. Yin, J. George, D.C. Guttridge, W. He, A. Wysong, M.S. Willis, M.E. Couch, Metabolomic analysis of cancer cachexia reveals distinct lipid and glucose alterations, Metabolomics 4 (3) (2008) 216–225.
[66] C. Grunfeld, K.R. Feingold, Metabolic disturbances and wasting in the acquired immunodeficiency syndrome, N. Engl. J. Med. 330 (1994) 1041–1046.
[67] S. Park, B. Goodpaster, J. Lee, L. Kuller, R. Boudreau, N. De Rekeneire, T. Harris, S. Kritchevsky, F. Tylavsky, M. Nevitt, Y. Cho, A. Newman, Excessive loss of skeletal muscle mass in older adults with type 2 diabetes, Diabetes Care 32 (11) (2009) 1993–1997.
[68] R.C. May, R.A. Kelly, W.E. Mitch, Mechanisms for defects in muscle protein metabolism in rats with chronic uremia. Influence of metabolic acidosis, J. Clin. Invest. 79 (4) (1987) 1099–1103.
[69] S.D. Anker, A.J.S. Coats, Cardiac cachexia: a syndrome with impaired survival and immune and neuroendocrine activation, Chest 115 (3) (1999) 836–847.
[70] S. Homer-Vanniasinkam, M.J. Gough, Role of lipid mediators in the pathogenesis of skeletal muscle infarction and oedema during reperfusion after ischaemia, Br. J. Surg. 81 (10) (1994) 1500–1503.
[71] U.N. Das, Interaction(s) between essential fatty acids, eicosanoids, cytokines, growth factors and free radicals: relevance to new therapeutic strategies in rheumatoid arthritis and other collagen vascular diseases, Prostaglandins Leukot. Essent. Fat. Acids 44 (4) (Dec. 1991) 201–210.
[72] B.H. Maskrey, I.L. Megson, P.D. Whitfield, A.G. Rossi, Mechanisms of resolution of inflammation: a focus on cardiovascular disease, Arterioscler. Thromb. Vasc. Biol. 31 (5) (2011) 1001–1006.
[73] B. Porro, P. Songia, I. Squellerio, E. Tremoli, V. Cavalca, Analysis, physiological and clinical significance of 12-HETE: a neglected platelet-derived 12-lipoxygenase product, J. Chromatogr. B 964 (Aug. 2014) 26–40.
[74] A.D. Southam, J.M. Easton, G.D. Stentiford, C. Ludwig, T.N. Arvanitis, M.R. Viant, Metabolic changes in flatfish hepatic tumours revealed by NMR-based metabolomics and metabolic correlation networks, J. Proteome Res. 7 (12) (2008) 5277–5285.